A VIRTUAL INTERNAL BOND MODEL FOR HYSTERETIC MEDIA

PIER PAOLO DELSANTO[1], VETURIA CHIROIU[2], TUDOR SIRETEANU[2], LIGIA MUNTEANU[2], MARIUS FLORINEL IONESCU[3]

Abstract. In this paper, the properties of the hysteretic media are investigated via the virtual internal bond model (VIB) derived from the hyperelasticity with the integration of the 6–12 Lennard-Jones atomic interacting potential.

Key words: hysteretic media, virtual internal bond model, hyperelasticity, Lennard-Jones potential.

1. INTRODUCTION

The randomized cohesive interactions between material particles play an important role in the predicting the dynamic fracture of materials [1]. A highly promising *virtual internal bond* (VIB) *model* in the simulation of fracture was proposed by [2–4] with the integration of the 6–12 Lennard-Jones atomic interacting potential. The VIB model differs from an atomistic model in that a cohesive force law is assumed to act between material particles which are not necessarily atoms. It also differs from a cohesive surface model in that, rather than imposing a cohesive law along a prescribed set of discrete surfaces, a randomized network of cohesive bonds is incorporated into the constitutive law of the material and the macroscopic collective behavior of this random bond network is obtained through the so-called Cauchy-Born rule. This rule consists in equating the strain energy function on the continuum level to the potential energy stored in the cohesive bonds due to an imposed deformation [5, 6]. The VIB model is derived from the hyperelastic principle [7] in order to integrate the macroscopic view of cohesive surfaces dispersed in a continuum background with the atomistic view of interatomic bonding.

In this paper, some properties of the hysteretic media are investigated by using a VIB model. In recent years, the relevance of nonlinear elastic techniques in the field of nondestructive evaluation (NDE) has been widely demonstrated [8, 9]. A 2D approach to the simulation of ultrasonic wave propagation in nonclassical

[1] INFM – Dip. di Fisica del Politecnico di Torino, Corso Duca degli Abruzzi 24, 10129 Torino

[2] Institute of Solid Mechanics of the Romanian Academy, str. Ctin Mille 15, 010141 Bucharest

[3] "Ion Neculce" Theoretical High School, str. Ion Neculce 2, Bucharest

nonlinear media is presented in [10]. The approach represents the extension to 2D of a 1D *Spring Model* introduced in [11], with the inclusion of a Preisach–Mayergoyz [12–15] space treatment of the interstitial regions between grains.

Recent development in the nonlinear theories has explored the general hyperelasticity theory which includes both nonlinear kinematics and nonlinear material behavior. The hyperelastic or Green elastic materials admit constitutive relations derived from a strain energy density functions [16, 17]. The hyperelastic material is a special case of a Cauchy elastic material [18–23]. All measures, such as strains and stresses, defined for linear isotropic elastic solids have to be recast in the context of a finite deformation theory. Details on the algorithms which can be used for determination of the elastic and viscoelastic constants by using the definition of the strain energy density function can be found in [24–31].

2. FORMULATION OF THE INTERNAL BOND MODEL FOR HYPERELASTIC MEDIA

We consider a homogeneous, isotropic, hyperelastic body of volume Ω_0 in the material or Lagrangean configuration and volume Ω in the spatial or Eulerian configuration. The body has a microstructure consisting of internal cohesive bonds between a network of randomly distributed material particles. The motion of the body may be described by the mapping

$$\mathbf{x} = \chi(\mathbf{X}, t), \tag{1}$$

where $\mathbf{x} = (x_1, x_2, x_3)$ is the position vector in the Eulerian configuration of the place occupied by the particle $\mathbf{X} = (X_1, X_3, X_3)$ in the Lagrangean configuration.

The mapping defined by a motion at any fixed time is called a deformation. Differentiating (1) for $t = \text{const.}$, it comes:

$$\mathrm{d}\mathbf{x} = \mathbf{F}\mathrm{d}\mathbf{X}, \quad \mathbf{F} = \operatorname{grad} \chi(\mathbf{X}, t), \tag{2}$$

where $\mathbf{F}$ is the deformation gradient, which can be expressed by $\mathbf{F} = \mathbf{1} + \mathbf{H}$, where $\mathbf{H} = \operatorname{grad} \mathbf{u}(\mathbf{x}, t)$ is the displacement gradient and $\mathbf{u}(\mathbf{x}, t)$ the displacement vector. Since χ is one-to one, $J = \det \mathbf{F} > 0$. Let denote $\mathbf{r}_{ij}^{(0)} = r_{ij}^{(0)} \mathbf{n}_{ij}^{(0)}$ the position vector of the bond between two material particles i and j, prior to deformation, with $r_{ij}^{(0)}$ the underformed bond length $r_{ij}^{(0)} = |\mathbf{r}_i - \mathbf{r}_j|$, where $\mathbf{r}_i$ and $\mathbf{r}_j$ are the positions vectors of the particle i and j. The $\mathbf{n}_{ij}^{(0)}$ is the unit vector. For particles i and j, the vector $\mathbf{r}_{ij}$ of the current bond after the deformation, becomes

$$\mathbf{r}_{ij} = \mathbf{F}\mathbf{r}_{ij}^{(0)}. \tag{3}$$

The current length $\mathbf{r}_{ij}$ of the bond is

$$r_{ij}(\mathbf{D}) = \sqrt{\mathbf{r}_{ij}\mathbf{r}_{ij}} = r_{ij}^{(0)}\sqrt{1+2\mathbf{n}_{ij}^{(0)}\mathbf{D}\mathbf{n}_{ij}^{(0)}}\,, \tag{4}$$

where $\mathbf{D} = \frac{1}{2}(\mathbf{F}^{\mathrm{T}}\mathbf{F} - \mathbf{1})$ is the finite strain tensor (Lagrangian strain tensor). An equivalent expression for $\mathbf{D}$ is: $\mathbf{D} = \frac{1}{2}\left(\mathbf{H} + \mathbf{H}^{\mathrm{T}} + \mathbf{H}\mathbf{H}^{\mathrm{T}}\right)$. In continuum mechanics, the total potential energy of the body is the integration over the volume V_0 of the strain energy density $W(\mathbf{D})$:

$$E_{tot} = \int_{\Omega_0} W(\mathbf{D})\mathrm{d}\Omega\,. \tag{5}$$

If the body is assumed to be consisted by a network of randomly distributed material particles, the total energy of the body admits the form

$$E_{tot} = \sum_i E_i\,, \tag{6}$$

where E_k is the energy of the i th material particle. The energy of the material particle i is defined by the internal cohesive bonds between this particle and its neighbour particles j [32]:

$$E_i = \frac{1}{2}\sum_{j\neq i} V_{ij}(r_{ij}, r_{ij}^{(0)})\,, \tag{7}$$

where V_{ij} is the pair potential of the bond between material particles i and j. To describe the energy stored in the bond between two particles, we use the 6-12 Lennard-Jones potential [33,34]:

$$V_{ij}(r_{ij}, r_{ij}^{(0)}) = V_{ij0}\left[\left(\frac{r_{ij}^{(0)}}{r_{ij}}\right)^{12} - 2\left(\frac{r_{ij}^{(0)}}{r_{ij}}\right)^{6}\right], \tag{8}$$

where r_{ij} is the current stretch length of the bond in the arbitrary direction $\mathbf{n}_{ij}^{(0)}$, and $r_{ij}^{(0)}$ the undeformed bond length. By using (4), the expression (8) becomes:

$$V_{ij}(\mathbf{D}) = V_{ij0}\left[\left(\frac{1}{\sqrt{1+2\mathbf{n}_{ij}^{(0)}\mathbf{D}\mathbf{n}_{ij}^{(0)}}}\right)^{12} - 2\left(\frac{1}{\sqrt{1+2\mathbf{n}_{ij}^{(0)}\mathbf{D}\mathbf{n}_{ij}^{(0)}}}\right)^{6}\right]. \tag{9}$$

From (5) we express the strain energy density $W(\mathbf{D})$ as

$$W(\mathbf{D}) = \frac{1}{\Omega_0} E_{tot} = \frac{1}{2!} C_{ijkl} D_{ij} D_{kl}, \tag{10}$$

where C_{ijkl} are the second-order elastic constants. By using (10), for given C_{ijkl} we can estimate the number of particle i needed to calculate (6) and the constants V_{ij0} from (8). The nonlinear constitutive equation of elastic materials can be written as [35]:

$$\mathbf{S} = \mathbf{F} \frac{\partial W(\mathbf{D})}{\partial \mathbf{D}}, \tag{11}$$

where $\mathbf{S}$ is the first Piola-Kirchhoff tensor related to the viscoelastic stress tensor $\mathbf{T}$ by: $\mathbf{S} = J\mathbf{T}\mathbf{F}^{-\mathrm{T}}$. The equation of motion can be written as:

$$\left(1 + \mu_v \frac{\partial}{\partial t}\right) \sum_m \frac{\partial S_{km}(\chi(\mathbf{X}, t))}{\partial X_m} = \rho_0 \frac{\partial^2 \chi(\mathbf{X}, t)}{\partial t^2}, \tag{12}$$

with $\rho_0 = \rho J$ the density of the undeformed material, $\chi(\mathbf{X}, t)$ given by (1) and μ_v is the coefficient of viscosity.

To understand the VIB model we present in the following the 1D case for $x = \chi(X,t)$ and we can define $\chi : [0,1] \to R$, $F(X) = \dfrac{\partial \chi}{\partial X} > 0$. Let L be the length of the underformed bond when unstretched, l the current length of the bond, and ξ the arbitrary bond orientation. Then, the stretch of an atomic bond from the undeformed bond in an arbitrary direction ξ can be expressed by (3) and (4) as [4]

$$l = LF, \quad F = \sqrt{1 + 2\xi^{\mathrm{T}} \mathbf{D} \xi},$$

where F is the 1D deformation gradient which maps the distance between particles from the reference L to the current l state. The 6–12 Lennard-Jones potential (8) and (9) can be written as

$$V(\mathbf{D}) = V_0 \left[\left(\frac{1}{\sqrt{1 + 2\xi^{\mathbf{T}} \mathbf{D} \xi}} \right)^{12} - 2 \left(\frac{1}{\sqrt{1 + 2\xi^{\mathbf{T}} \mathbf{D} \xi}} \right)^{6} \right].$$

The equation of motion (12) can be written as

$$\frac{\partial}{\partial X} \left[\sigma \left(\frac{\partial \chi}{\partial X} \right) \right] + \mu_v \frac{\partial^3 \chi}{\partial t \partial^2 X} = \rho_0 \frac{\partial^2 \chi}{\partial t^2},$$

where $\sigma\left(\frac{\partial\chi}{\partial X}\right)=12\alpha\left[\frac{1}{F^7}-\frac{1}{F^{13}}\right]$, with α a constant and $v(X,t)$ the velocity.

The boundary conditions and the initial conditions are:

$$\chi(0,t)=0\,,\ \ \chi(1,t)=a\,,\ \ \chi(X,0)=\chi_0(X)\,,\ \ \frac{\partial\chi}{\partial t}(X,0)=v_0(X)\,.$$

For a thermo-hyperelastic material, we must define four constitutive laws giving the strain energy density $W(\mathbf{D})$, the first Piola-Kirchhoff tensor $\mathbf{S}$ related by the viscoelastic stress tensor $\mathbf{T}$ by $\mathbf{S}=J\mathbf{T}\mathbf{F}^{-\mathrm{T}}$, the specific entropy η and the heat flux $\mathbf{q}$ at each material point $\mathbf{X}$ in terms of the finite strain tensor $\mathbf{D}=\frac{1}{2}(\mathbf{F}^{\mathrm{T}}\mathbf{F}-\mathbf{1})$, the absolute temperature θ and the temperature gradient $\mathbf{g}=\mathrm{Grad}\,\theta$ at $\mathbf{X}$, as follows:

$$W=\frac{1}{\Omega_0}E_{tot}=W(\mathbf{D},\theta,\mathbf{g})\,,\ \ \mathbf{S}=\mathbf{S}(\mathbf{D},\theta,\mathbf{g})=\mathbf{F}\frac{\partial W(\mathbf{D},\theta,\mathbf{g})}{\partial\mathbf{D}}\,,$$

$$\eta=\eta(\mathbf{D},\theta,\mathbf{g})=-\frac{\partial W(\mathbf{D},\theta,\mathbf{g})}{\partial\theta}\,,\ \ \mathbf{q}=\mathbf{q}(\mathbf{D},\theta,\mathbf{g})\,, \tag{13}$$

where the heat flux must obey the heat conduction inequality $\mathbf{q}(\mathbf{D},\theta,\mathbf{g})\,\mathrm{grad}\,\theta\le 0$.

3. THE VIB EQUATION WITH HYSTERESIS

Let us consider a system whose state is characterized by two scalar variables, u and w, confined to a set $L\subset R^2$. Assume that $\forall t\in[0,T]$, the function $w(t)$ depends on the previous evolution of u (memory effect) and on the initial state w_0, such as:

$$w(t)=A(u,w_0)(t)\,,\ \ \forall t\in[0,T]\,, \tag{14}$$

where $A(u,w_0)$ is a memory operator defined in a Banach space of time-dependent functions. If $(u(0),w_0)\in L$ then $A(u,w_0)(0)=w_0$. The memory operator is causal, $\forall(u_1,w_0),(u_2,w_0)\in\mathrm{D}(A)$ with $u_1=u_2$ in $[0,T]$, then $A(u_1,w_0)(t)=A(u_2,w_0)(t)$.

Equation (14) can exhibit singularities in a finite time. The generalized concept of weak solutions with allowed discontinuities must be defined in order to be able to obtain the solutions of a given PDEs [36–39].

A discontinuous hysteresis operator is the relay operator [40–43]:

Definition of the Relay Operator (Visintin). Let us denote by $C_r^0([0, T])$ the space of continuous functions on the right in $[0, T]$. For any pair $\rho := (\rho_1, \rho_2) \in R^2$ the (*delayed*) *relay operator* is defined as

$$h_\rho : C^0([0, T]) \times \{-1, 1\} \to BV(0, T) \cap C_r^0([0, T]) . \tag{15}$$

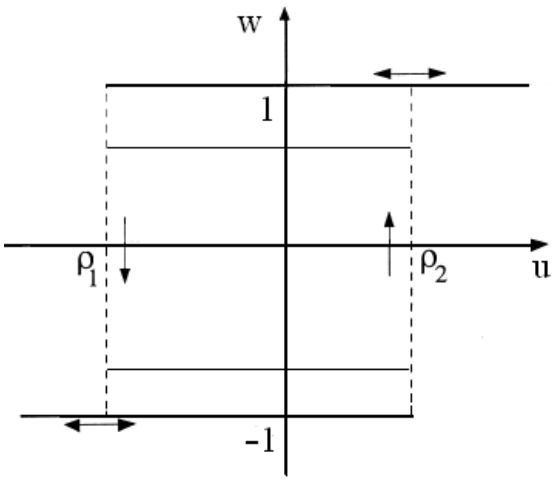

Fig. 1 – Relay operator.

The operator h_ρ is not closed. For any $u \in C^0([0,T])$ and $\forall \xi \in \{-1, 1\}$, we set

$$X_t := \{\tau \in]0,t] : u(\tau) = \rho_1 \text{ or } \rho_2\} ,$$

for any $t \in [0, T]$, and define the function $w = h_\rho(u, \xi) : [0,T] \to \{-1, 1\}$ as follows:

$$w(0) := \begin{cases} -1 & \text{if } u(0) \le \rho_1, \\ \xi & \text{if } \rho_1 < u(0) \le \rho_2, \\ 1 & \text{if } u(0) \ge \rho_2, \end{cases} \tag{16}$$

$$w(t) := \begin{cases} -1 & \text{if } X_t \neq \varnothing \text{ and } u(\max X_t) = \rho_1 \quad \forall t \in [0, T], \\ 1 & \text{if } X_t \neq \varnothing \text{ and } u(\max X_t) = \rho_2, \end{cases} \tag{17}$$

with $w(t) = w(0)$ if $X_t = \varnothing$. The conditions (14) and (15) assure the uniqueness of w in $[0, T]$. The jumps of w up to 1 and down to -1 are illustrated in Fig. 1.

In order to associate the relay operator to PDEs, it is of interest to deal with the closure of (15). The relay operator has to be extended by allowing w to have intermediate values between -1 and 1.

Therefore, for any $u \in C^0([T])$ and $\xi \in [-1, 1]$, a set $w \in k_\rho(u, \xi)$ is introduced if and only if w is measurable in $[0, T]$ and

$$w(0) = \begin{cases} -1 & \text{if } u(0) < \rho_1, \\ \{-1, \xi] & \text{if } u(0) = \rho_1, \\ \xi & \text{if } \rho_1 < u(0) < \rho_2, \\ [\xi, 1] & \text{if } u(0) = \rho_2, \\ 1 & \text{if } u(0) > \rho_2, \end{cases} \tag{18}$$

$$w(t) := \begin{cases} -1 & \text{if } u(t) < \rho_1, \\ [-1, 1] & \text{if } \rho_1 \le u(t) \le \rho_2, \\ 1 & \text{if } u(0) > \rho_2, \end{cases} \tag{19}$$

with additional remarks: (*i*) if $u(t) \neq \rho_1, \rho_2$ then w is constant in a neighbourhood of t; (*ii*) if $u(t) = \rho_1$ then w is nonincreasing in a neighbourhood of t; and if $u(t) = \rho_2$ then w is nondecreasing in a neighbourhood of t.

So, the function $w \in BV(0, T)$ exists for

$$k_\rho : C^0([0,T]) \times \{-1, 1\} \to P(BV(0, T)). \tag{20}$$

The equation VIB (12) with hysteresis can be written as

$$\begin{gathered} \left(1 + \mu_v \frac{\partial}{\partial t}\right) \sum_m \frac{\partial S_{km}(\chi(\mathbf{X}, t))}{\partial X_m} = \rho_0 \frac{\partial^2 \chi(\mathbf{X}, t)}{\partial t^2}, \\ \chi(\mathbf{X}, t) = u(\mathbf{X}, t) + w(\mathbf{X}, t), \end{gathered} \tag{21}$$

with $\rho_0 = \rho J$ the density of the undeformed material, $\chi(\mathbf{X}, t)$ given by (1), μ_v is the coefficient of viscosity, and

$$w(\mathbf{X}, t) = A(u(\mathbf{X}, t), w_0), \quad w_{,t} \in \phi(u, w), \quad w(\mathbf{X}, 0) = w_0(\mathbf{X}) \quad \text{in } (0, T), \tag{22}$$

where $\gamma_l(u) = u + r$, $\gamma_r(u) = u - r$, with $r \ge 0$ a parameter, $u(t)$ a continuous input function on $[0, T]$ and $w_{r0} \in [-r, r]$ an initial state, and

$$\phi(u,w)=\begin{cases}\{\infty\} \text{ if } w<\inf\gamma_r(u),\\ [0,+\infty] \text{ if } w\in\gamma_r(u)\setminus\gamma_l(u),\\ \{0\} \text{ if } \sup\gamma_r(u)<w<\inf\gamma_l(u),\\ [-\infty,0] \text{ if } w\in\gamma_l(u)\setminus\gamma_r(u),\\ \{-\infty\} \text{ if } w>\sup\gamma_r(u),\\ [-\infty,+\infty] \text{ if } w\in\gamma_l(u)\cap\gamma_r(u).\end{cases} \tag{23}$$

4. APPLICATIONS

The first example is a virtual experiment performed on an AlMgSi aluminium alloy plate $10\times5\ \text{cm}^2$ [10] with elastic constants $C_{iiii}=110.5$ GPa, $\lambda=C_{iijj}=58.5$ GPa, $\mu=C_{ijij}=26$ GPa, density $\rho_0=2{,}700\ \text{kg/m}^3$ and the coefficient of viscosity $\mu_v=0.1$ kg/ms.

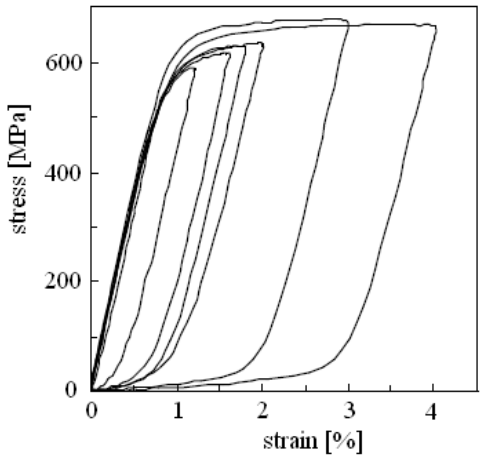

Fig. 2 – Stress-strain loop for the aluminium alloy.

The numerical experiments suggest that the viscosity cannot be too small in order to control the stability of the problem. We inject a cycle longitudinal sinusoidal plane wave from the left side of the specimen with frequency 0.6 MHz and amplitude set in order to give a strain of the order of 10^{-9} m. Fig. 2 presents a stable stress-strain hysteresis loop, measured at different values of strain amplitude, plotted in relative coordinates corresponding to a translation of the loops ascending branches in such a way that their tips coincide at the positions of the load reversal in compression. Fig. 3 illustrates the 3D plots of the wave amplitude with various

wave fronts. The results agree with results reported in [10] based on an extension to 2D of the 1D *Spring Model*. However, it is necessary to perform quantitative comparisons with the experimental results, in order to confirm the predictive value of the model, either in its simplified 1D form or in a more general 2D or 3D version.

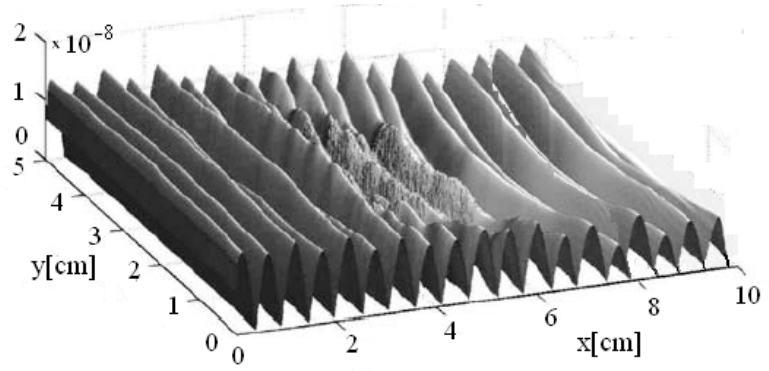

Fig. 3 – 3D plots of the wave amplitude.

The second example concerns a virtual experiment performed on a NiTi ribbon of length $= 1$ m, width $= 0.1$ m and thickness $= 1.27\times10^{-3}$ m, with elastic constants $\lambda^{A,M} = C_{iijj} = 28.26$ GPa, $\mu^{A,M} = C_{ijij} = 18.85$ GPa (A counts for the austenite and M for the martensite), density $\rho_0 = 6{,}450$ kg/m^3, coefficient of linear thermal expansion $12.5\times10^{-6}\,1/°\text{C}$ for both phases, thermal conductivity 18 W/m °C for austenite and 8.5 W/m °C for martensite, slope of stress versus temperature 13.5 MPa/ °C for both phases, the heat capacity $= 5.44\times10^{6}$ °C J m^{-3} and the coefficient of viscosity $\mu_v = 0$.

Shape memory alloys (SMAs) are materials capable of very large recoverable inelastic strain (of the order of 10 %). The source of this mechanical behaviour is a crystalline phase transformation between the austenite (A) and martensite (M). There are two main phases associated with the shape memory effect, austenite at the high temperature phase and martensite, at the low temperature phase [44]. The input variable is temperature $T(t)$ and the output is the strain $\varepsilon(t)$. Fig. 4 shows the major loop of a NiTi sample obtained by applying the VIB model. Fig. 4 also shows the experimental and theoretical results obtained by Ktena and Manassis [45] via the Preisach formalism. From Fig. 4 we can conclude that VIB is a good model.

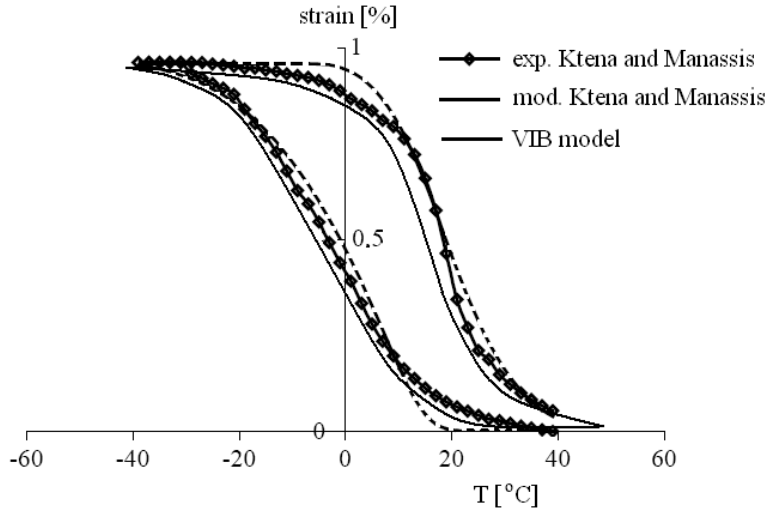

Fig. 4 – Hysteresis major loop for a NiTi ribbon.

The last example is a virtual experiment performed on the cyclic twisting of a cylindrical rubber membrane. Both edges of the cylinder are attached to rigid discs as depicted in Fig. 5. The height of the cylinder remains constant during the rotation of the lower disc. The diameter of the membrane is $D = 100$ mm, the height $H = 300$ mm, the thickness $h = 0.1$ mm, $\lambda = C_{iijj} = 0.0577$ GPa, $\mu = C_{ijij} = 0.0385$ GPa, the density $\rho_0 = 1{,}100$ kg/m^3 and the coefficient of viscosity $\mu_v = 0.1$ kg/ms.

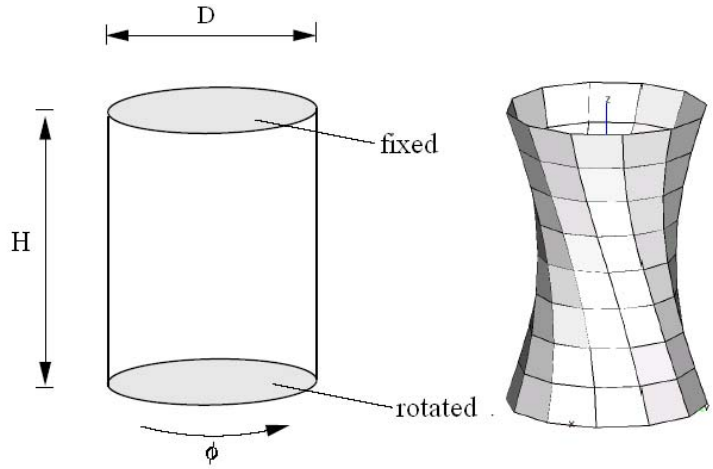

Fig. 5 – The scheme of the twist of a cylindrical rubber membrane.

Fig. 6 shows the major loop of the membrane obtained by applying the VIB model. One of the peculiarities of this hysteresis is the non-monotonic shape. At a certain value of the strain, the stress is decreasing rather than increasing. The material becomes more compliant and further deformation appears without raising the stress. Finally, the stress stabilizes and then starts increasing again, indicating less compliance to deformation. This apparent strain hardening is attributed to crystalization phenomena in rubber-like materials. Similar shapes for hysteresis loops are found in [46] for natural latex and rubbers-like materials.

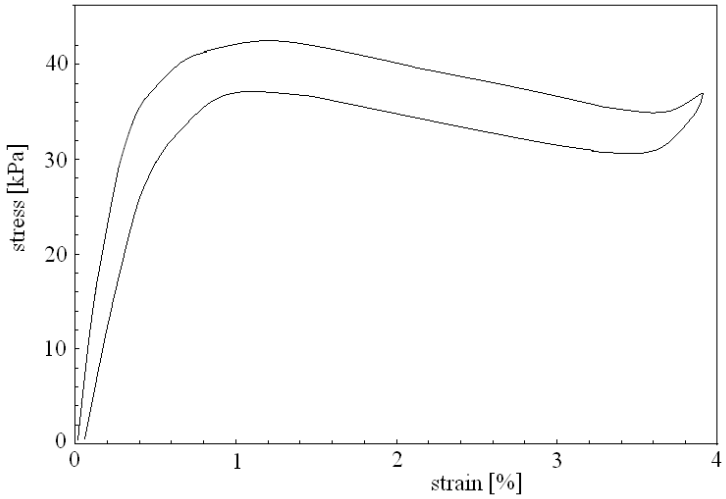

Fig. 6 – Stress-strain loop for cylindrical rubber membrane.

4. CONCLUSIONS

In this paper, the hysteretic media are investigated by using a virtual internal bond model (VIB) derived from the hyperelasticity with the integration of the 6–12 Lennard–Jones atomic interacting potential. In this model the cohesive forces are assumed to act between material particles which are not necessarily atoms. A randomized network of cohesive bonds is incorporated into the constitutive law of the material and the macroscopic collective behavior of this random bond network is obtained through the so-called Cauchy–Born rule. The VIB model is derived from the hyperelastic principle in order to integrate the macroscopic view of cohesive surfaces dispersed in a continuum background with the atomistic view of interatomic bonding. Three virtual experiments are performed for different materials, such as the aluminium alloy, the NiTi shape memory alloys and rubbers.

The intention of this paper was to gain an insight of the interaction mechanisms involved in the hysteresis phenomena. We can conclude that the

hysteresis behaviour of materials is modelled accurately, and the computational tool is easy and efficient to be applied.

Acknowledgments. We gratefully acknowledge Dr. Marco Scalerandi from Politecnico di Torino, Dip di Fisica and Prof. Dan Iordache from Politehnica University from Bucharest for fruitful discussions on the atomic extension of the hysteresis models.

Received on December 10, 2010

REFERENCES

1. GAO, H., KLEIN, P., *A quasicontinuum cohesive model with randomized internal cohesive bounds*, Preprint, Division of Mechanics and Computation, Stanford University, March 1997.
2. GAO, H., KLEIN, P., *Numerical simulation of crack growth in an isotropic solid with randomized internal cohesive bonds*, J. Mech. Phys. Solids, **46**, pp. 187–218, 1998.
3. LIN, P., *A nonlinear wave equation of mixed type for fracture dynamics*, Research Report No. 777, Department of Mathematics, The National University of Singapore, August 2000.
4. LIN, P., SHU, C-W. *Numerical solution of a virtual internal bond model for material fracture*, Physica D: Nonlinear Phenomena, **167**, *1-2*, pp. 101–121, 2002.
5. BORN, M., HUANG, K., *Dynamical theory of the crystal lattices,* Oxford University Press, Oxford, 1954.
6. MILSTEIN, F., *Review: theoretical elastic behaviour at large strains*, J. Math. Sci., **15**, pp. 1071–1084, 1980.
7. OGDEN, R.W., *Non-Linear Elastic Deformations*, Dover, 1984.
8. VAN DEN ABEELE, K., CARMELIET, J., TENCATE, J., JOHNSON, P., *Nonlinear elastic wave spectroscopy (NEWS) techniques to discern material damage. Part I*, Res. Nondestr. Eval., **12**, pp. 17–30, 2000.
9. VAN DEN ABEELE, K., CARMELIET, J., TENCATE, J., JOHNSON, P., *Nonlinear elastic wave spectroscopy (NEWS) techniques to discern material damage. Part II*, Res. Nondestr. Eval., **12**, pp. 31–42, 2000.
10. DELSANTO, P.P., GLIOZZI, A.S., HIRSEKORN, M., NOBILI, M., *A 2D spring model for the simulation of ultrasonic wave propagation in nonlinear hysteretic media*, Ultrasonics, **44**, pp. 279–286, 2006.
11. DELSANTO, P.P., SCALERANDI, M., *A spring model for the simulation of the propagation of ultrasonic pulses through imperfect contact interfaces*, J. Acoust. Soc. Am., **104**, *5*, 1998.
12. HOLCOMB, D., *Memory, relaxation and microfacturing in dilatant rock*, J. Geophys. Res., **86**, pp. 6235–6245, 1981.
13. MCCALL, K., GUYER, R., *A new theoretical paradigm to describe hysteresis, discrete memory and nonlinear elastic wave propagation in rock*, Nonlinear Proc. Geophys, **3**, p.89, 1996.
14. PREISACH, F., *Uber die magnetische nachwirkung*, Zeitschrift fur Physik, **94**, pp. 277–302, 1935.
15. MAYERGOYZ, I., *Mathematical Models of Hysteresis*, Springer, New York, 1991.
16. RIVLIN, R.S., *Large Elastic Deformations of Isotropic Materials IV. Further Developments of the General Theory*, Phil.Trans.Roy.Soc., **A241**, *835*, pp. 379–397, 1948.
17. MOONEY, M., *A Theory of Large Elastic Deformation*, J.Appl.Phys, **11**, *9*, pp. 582–592, 1940.
18. ERINGEN, A.C., *Mechanics of Continua*, John Wiley and Sons, New York, 1967.
19. ERINGEN, A.C., *Nonlinear theory of Continuous Media*, McGraw-Hill, New York, 1962.
20. MALVERN, L.W., *Introduction to the Mechanics of a Continuum Medium*, Prentice-Hall, Englewood Cliffs, N.J., 1969.

21. GREEN, A.E., ADKINS, J.E., *Large Elastic Deformations*, Oxford University Press, London, 2nd edition, 1970.
22. GREEN, A.E., ZERNA, W., *Theoretical Elasticity*, Oxford University Press, London, 2nd edition, 1968.
23. TRUESDELL, C., NOLL, W., *The Nonlinear Field Theories of Mechanics*, Springer-Verlag, Berlin, 2nd edition, 1970.
24. CHIROIU, C., MUNTEANU, L., CHIROIU, V., DELSANTO, P.P., SCALERANDI, M., *A genetic algorithm for determining of the elastic constants of a monoclinic crystal*, Inverse Problems, **16**, pp. 121–132, 2000.
25. CHIROIU, C., DELSANTO, P.P., SCALERANDI, M., CHIROIU, V., SIRETEANU, T., *Subharmonic generation in piezoelectrics with Cantor-like structure,* Journal of Physics D: Applied Physics, **34**, *3*, pp. 1579–1586, 2001.
26. CHIROIU, V., CHIROIU, C., RUGINA, C., DELSANTO, P.P., SCALERANDI, M., *Propagation of ultrasonic waves in nonlinear multilayered media,* Journal of Computational Acoustics, **9**, *4*, pp. 1633–1646, 2001.
27. CHIROIU, V., DELSANTO, P.P., MUNTEANU, L., RUGINA, C., SCALERANDI, M., *Determination of the second-and third-order elastic constants in Al from the natural frequencies*, Journal of the Acoustical Society of America, **102**, *1*, 1997.
28. SCALERANDI, M., DELSANTO, P.P., CHIROIU, C., CHIROIU, V., *Numerical simulation of pulse propagation in nonlinear 1-D media*, Journal of the Acoustical Society of America, **106**, *1*, pp. 2424–2430, 1999.
29. MUNTEANU, L., CHIROIU, C., CHIROIU, V., *Nonlinear dynamics of the left ventricle*, Physiological Measurement, Institute of Physics Publishing, **23**, pp. 417–435, 2002.
30. CHIROIU, C., PREVOROVSKY, Z., MUNTEANU, L., CHIROIU, V., *A genetic algorithm for determination of the material constants of a viscoelastic monoclinic crystal*, Proc. of the Euromech symposium 419 Elastic waves in Nondestructive Testing, October 2000, Praga.
31. DELSANTO P. P., PROVENZANO V., H. UBERALL, *Coherency strain effects in metalic bilayers*, J. Phys.: Condens. Matter, *4*, pp. 3915–3928, 1992.
32. CURTIN, W.A., MILLER, F., *Atomistic continuum coupling in computational material science*, Modelling and Simulation in Materials Science and Engineering, **11**, R33–R68, 2003.
33. LENNARD-JONES, J. E., *On the Determination of Molecular Fields*, Proc. R. Soc. Lond. A, **106**, *738*, pp. 463–477, 1924.
34. RAFII-TABAR, H., *Modelling the nano-scale phenomena in condensed matter physicsvia computer-based numerical simulations*, Phys. Rep., **325**, pp. 239–310, 2000.
35. TEODOSIU, C., *Elastic models of crystal defects*, Ed. Acad., Springer-Verlag, 1982.
36. IONESCU, M.F., CHIROIU, V., DUMITRIU, D., MUNTEANU, L., *A special class of DRIP media with hysteresis*, (in press) 2011.
37. PREDA, V., IONESCU, M.F., CHIROIU, V., DUMITRIU, D., *A Preisach model for the analysis of the hysteretic phenomena*, Rev. Roum. Sci. Techn. – Méc. Appl., **55**, *3*, 2010.
38. IONESCU, M.F., MUNTEANU, L., CHIROIU, L., *On the hysteresis operators,* Proc. of the Romanian Academy, Series A: Mathematics, Physics, Technical Sciences, Information Science, (in press) 2001.
39. GLIOZZI, A.S., MUNTEANU, L., SIRETEANU, T., CHIROIU, V., *An identification problem from input-output data*, Rev. Roum. Sci. Techn. – Méc. Appl., **55**, *3*, 2010.
40. VISINTIN, A., *Quasi-linear hyperbolic equations with hysteresis*, Ann. Inst. H. Poincaré, Nonlinear Analysis, **19**, pp. 451–476, 2002.
41. VISINTIN, A., *Differential Models of Hysteresis.* Springer-Verlag, Berlin 1995.
42. VISINTIN, A., *Homogenixation of some models of hysteresis*, Physica B, **403**, pp. 245–249, 2008.
43. KOPFOVÁ, J., *Entropy condition for a quasilinear hyberbolic equation with hysteresis*, Differential and Integral Equations, **18**, *4*, pp. 451–467, 2004.

44. MIHAILESCU, M., CHIROIU, V., *Advanced mechanics on shells and intelligent structures*, Editura Academiei Române, Bucharest, 2004.
45. KTENA, A., MANASSIS, C., *Preisach Hysteresis Modeling and Applications,* Proceedings of the 2006 IASME International Conference on Energy & Environmental Systems, Chalkida, Greece, May 8-10, 2006, pp. 232–236.
46. MAKINO, A., HAMBURGEN, W.R., FITCH, J.S., *Fluoroelastomer pressure pad design for microelectronic applications*, Western Research Laboratory, Research Report 93/7, 1993.